FEBS Letters 552 (2003) 86–90 FEBS 27622

From the first to the second domain of gelsolin: a common path on the surface of actin?[1]

Edward Irobi[a], Leslie D. Burtnick[b,2], Dunja Urosev[b,2], Kartik Narayan[a], Robert C. Robinson[a,*]

[a] *Department of Medical Biochemistry and Microbiology, Uppsala University, BMC, Box 582, 751 23 Uppsala, Sweden*
[b] *Department of Chemistry and Center for Blood Research, University of British Columbia, Vancouver, BC, Canada V6T 1Z1*

Received 22 May 2003; accepted 1 June 2003

First published online 29 August 2003

Edited by Amy McGough

Abstract We present the 2.6 Å resolution crystal structure of a complex formed between G-actin and gelsolin fragment Met25–Gln160 (G1+). The structure differs from those of other gelsolin domain 1 (G1) complexes in that an additional six amino acid residues from the crucial linker region into gelsolin domain 2 (G2) are visible and are attached securely to the surface of actin. The linker segment extends away from G1 up the face of actin in a direction that infers G2 will bind along the same long-pitch helical strand as the actin bound to G1. This is consistent with a mechanism whereby G2 attaches gelsolin to the side of a filament and then directs G1 toward a position where it would disrupt actin–actin contacts. Alignment of the sequence of the structurally important residues within the G1–G2 linker with those of WH2 (WASp homology domain 2) domain protein family members (e.g. WASp (Wiscott–Aldridge syndrome protein) and thymosin β4) suggests that the opposing activities of filament assembly and disassembly may exploit a common patch on the surface of actin.

Key words: Gelsolin; Actin; WH2 domain; Crystal structure

1. Introduction

Cell movement involves spatial and temporal control of actin polymerization and actin filament recycling at the leading edge of a moving cell (reviewed in [1]). A number of indispensable protein-elicited activities are required to maintain a pool of actin in a state able to repetitively provide propulsion by means of actin polymerization [2]. These activities are: (a) actin nucleation, ab initio, via the arp2/3 complex or through uncapping of existing filaments; (b) arp2/3 activation, by WASp (Wiscott–Aldridge syndrome protein) family members; (c) actin capping, to prevent wasteful polymerization (e.g. by capping protein, capG or gelsolin); (d) filament severing, to disassemble redundant filaments (e.g. by cofilin); and nucleotide exchange, to prepare the disassembled actin monomers for repolymerization (e.g. by profilin).

Gene knockout and overexpression experiments have firmly identified gelsolin to be a locomotion enhancer in fast moving cells [3]. Gelsolin is able to terminate actin filament assembly and regulate actin filament disassembly through cooperative interactions among its similarly, yet independently, folded set of six domains, G1–G6 (reviewed in [4,5]). The Ca^{2+}-free, inactive form of gelsolin is folded into a compact globule in which the binding sites for both G- and F-actin are hidden [6]. In this structure, the packing of G1–G3 (the first half of gelsolin) is similar to that of G4–G6 (the second half of the protein). This infers that the two halves of activated gelsolin, tethered by a long linking peptide between G3 and G4, act in a semi-autonomously fashion to bind to adjacent actin monomers at the barbed end of an actin filament [7].

G2 in the first half of gelsolin is the sole F-actin binding domain in the protein [4,5]. The structure of G4–G6 bound to actin yields a plausible model for the capped barbed end of F-actin [7]. However, it is clear that the dynamics of severing require G2 to be oriented in a position quite different from that found for its analog, G5, in the activated second half of gelsolin. So, although the structures of the two halves of gelsolin are similar in the inactive state [6], they are expected to be significantly different once activated. Several investigators have focused attention on the linker between G1 and G2 as a possible pivot point that would allow G2 to move to a position that would be consistent with its role as the F-actin binding domain of gelsolin [8–12]. The terminal residues of G1 in the structure of G1 bound to monomeric actin [13] point in a direction that suggests G2 may bind to a G1-type site on actin, but one unit away on the same strand of the long-pitch actin helix [8]. Severing can be viewed as proceeding through activation of gelsolin to expose its F-actin binding site on G2, binding to the side of a filament, and subsequent insertion of G1 into its binding site. Interaction of G4 from the second half of gelsolin at the same location on an actin unit across the filament axis completes the severing process and provides a tight cap over the barbed end of the freshly cut filament.

*Corresponding author. Fax: (46)-18-4714975; Website: http://www.imbim.uu.se/forskning/robinsonresearch.html.
E-mail addresses: edwardirobi@hotmail.com (E. Irobi), burtnick@chem.ubc.ca (L.D. Burtnick), dunja_urosev@hotmail.com (D. Urosev), kartik@princeton.edu (K. Narayan), bob.robinson@imbim.uu.se (R.C. Robinson).

[1] Data deposition: The atomic coordinates and merged structure factors have been deposited in the Protein Data Bank, www.rcsb.org (PDB ID code 1P8Z).
[2] Website: http://www.chem.ubc.ca/personnel/faculty/burtnick.

Abbreviations: G1+, human gelsolin fragment Met25 to Gln160; G1, gelsolin domain 1; G2, gelsolin domain 2; WASp, Wiscott–Aldridge syndrome protein; WIP, WASp interacting protein; WH2, WASp homology domain 2; WAVE, WASp family verprolin homologous protein; CAP, adenyl cyclase-associated protein

0014-5793/03/$22.00 © 2003 Published by Elsevier B.V. on behalf of the Federation of European Biochemical Societies.
doi:10.1016/S0014-5793(03)00934-7

Experimental evidence to support this model comes from electron cryomicroscopic studies of G2–G6 bound to F-actin [9]. Reconstruction based on averaging of images leads to a low-resolution model in which G2 is attached to two actin monomers in the same long-pitch helix, with G3 pointing away at an angle to higher radial distances. Density in the model diminishes significantly beyond G3, but allows the inference that the remaining domains could reach and bind to an actin across the filament from the site of contact with G2. The model can be extended to accommodate G1 making contact with subdomains 3 and 4 of the next actin along the filament axis at its previously identified binding site [13]. To accommodate this, some extension of the peptide linker between G1 and G2 would be necessary relative to the inactive form of gelsolin.

In this work, our goal was to provide higher-resolution testing of the validity of the hypothesis that G2 and G1 bind to adjacent units on the same long-pitch actin helix. To do this, we elucidated the structure of a fragment of gelsolin bound to actin that corresponds to G1 as used by McLaughlin et al. [13] but incorporated an additional six residues from the N-terminal section of G2, sufficient to render the fragment more active with regard to the severing of F-actin [14]. The structure clearly supports the hypothesis that G2 in activated gelsolin will bind along the side of F-actin and position G1 to insert between that actin bound to G2 and the actin unit one step away in the same long-pitch helix. A surprising finding, however, is that the novel actin-binding motif has analogs in the WH2 (WASp homology domain 2) domain family of proteins. Some members of this family of proteins (WASp, WIP (WASp interacting protein), etc.) are involved in the actin assembly machinery (reviewed in [15]). Thus actin-binding proteins with directly contrasting activities may employ structurally overlapping mechanisms.

2. Materials and methods

G-actin was prepared from an acetone powder of rabbit skeletal muscle powder [16] and further fractionated by gel filtration on Sephacryl S-300 (Amersham Biosciences). cDNA encoding full-length human plasma gelsolin was a generous gift from Dr. H.L. Yin (Texas Southwestern Medical Center, Dallas, TX, USA). The gene fragment coding for human gelsolin amino acid residues 25–160 (G1+) was engineered by polymerase chain reaction into a vector designed to encode an eight-histidine tag, followed by a thrombin cleavage site, ahead of the N-terminus of G1+. Val26 is the N-terminal residue of human cytoplasmic G1 and Met25 is the final residue of the N-terminal extension that differentiates the cytoplasmic and extracellular forms of gelsolin. The identity of the construct was verified by DNA sequencing with an ABI model 310 DNA sequencer. G1+ was expressed in *Escherichia coli* BL-21 Gold (DE3) cells grown in 2 l flasks at 37°C in Terrific Broth containing 50 μg/ml kanamycin. The temperature was reduced to 30°C after induction with isopropyl-β-D-thiogalactopyranoside (MBI Fermentas) at 1 mM and growth was allowed to continue for an additional 210 min. The cells were then harvested and centrifuged for 20 min at 4000 rpm at 4°C. The pellets were stored at −20°C. Lysis of the cells was carried out by a freeze–thaw procedure in the presence of 300 mM NaCl, 10 mM imidazole, 10 mM Tris–HCl, pH 8.0. Lysozyme was added to a final concentration of 1 μg/ml with stirring at 4°C for 30 min. Sonication was used to further break down bacterial cell walls and release protein. The suspension was clarified by centrifugation at 20 000 × *g* at 4°C for 30 min. 1.5 ml of Ni-NTA (Qiagen) beads was added to the supernatant, which was rocked continuously at 4°C for 30 min. The Ni-NTA beads were centrifuged at 1000 × *g* at 4°C for 5 min and resuspended in 300 mM NaCl, 20 mM imidazole, 10 mM Tris–HCl, pH 8.0. The beads were washed until no protein could be detected in the flowthrough using the Bio-Rad protein assay. G1+ was eluted using 300 mM NaCl, 250 mM imidazole, 10 mM Tris–HCl, pH 8.0. The His tag was cleaved by addition of thrombin and dialysis overnight at 4°C against buffer A (2 mM Tris–HCl, 0.2 mM ATP, 0.2 mM $CaCl_2$, 1 mM NaN_3, 0.5 mM dithiothreitol, pH 7.6). Subsequently, thrombin was removed by treatment with benzamidine Sepharose (Amersham Biosciences). The Sepharose beads were centrifuged at 1000 × *g* at 4°C for 5 min and the supernatant was passed through a 1 ml Ni-NTA column. The flowthrough was collected and further purified by passage through a 90 × 2.5 cm column of Superdex 200 (Amersham Biosciences) using 150 mM NaCl, 10 mM Tris–HCl, pH 8.0. Mass spectrometric analysis of protein excised from electrophoretic gels confirmed the protein to be the desired recombinant G1+ (M_r = 14 956.8). To form the complex between G1+ and actin, $CaCl_2$ was added to the recombinant G1+ solution to a final concentration of 0.1 mM. Then, $G1^+$ was added at a 1.5-fold molar excess over G-actin to drive formation of the complex. G1+/actin complex was purified by a second passage through the Superdex 200 column in buffer A. Fractions were examined by SDS–PAGE and those containing the complex were pooled and concentrated to 15.0 mg/ml.

Crystals of G1+/actin were obtained by the vapor diffusion method at 20°C in 3 μl hanging drops containing a 2:1 (v/v) mixture of the protein solution (at 15 mg/ml) and precipitant, 12.5% (v/v) polyethyleneglycol 400 (Fluka Chemie), 0.1 M NaOAc buffer, pH 5.0, 10 mM $CdCl_2$. Crystals appeared on the fifth day. Data were collected at 100 K at beamline ID-29 at the European Synchrotron Radiation Facility in Grenoble. Data were indexed and scaled in the programs

Table 1
Data collection and refinement statistics

Wavelength (Å)	1.0052
Space group	$P3_112$
Unit cell	$a = b = 114.2$, $c = 93.8$ Å $\alpha = \beta = 90°$, $\gamma = 120°$
Resolution range (Å)	20.0–2.6 (2.69–2.60)
Unique reflections	21 012 (2115)
Redundancy	3.6 (3.9)
Completeness (%)	97.4 (99.2)
Average I/σ	14.3
R_{merge}[a] (%)	7.7 (26.7)
R_{cryst}[b] (%)	20.8 (24.8)
R_{free}[c] (%)	26.3 (33.1)
Non-hydrogen atoms (ATP, cadmium ions, calcium ions, water)	4031 (31, 3, 1, 184)
G1+ consists of residues	26–156
Actin consists of residues	6–39, 51–370
Mean temperature factor (G1+, actin, ATP) (Å^2)	39.8, 35.8, 43.8
RMS deviation bonds (Å)	0.011
RMS deviation angles (°)	1.58

[a] R_{merge} $(\Sigma|I-\langle I\rangle|/\Sigma\langle I\rangle)$.
[b] R_{cryst} $(\Sigma||F_o|-|F_c||/\Sigma|F_o|$.
[c] Based on 5% of the data.

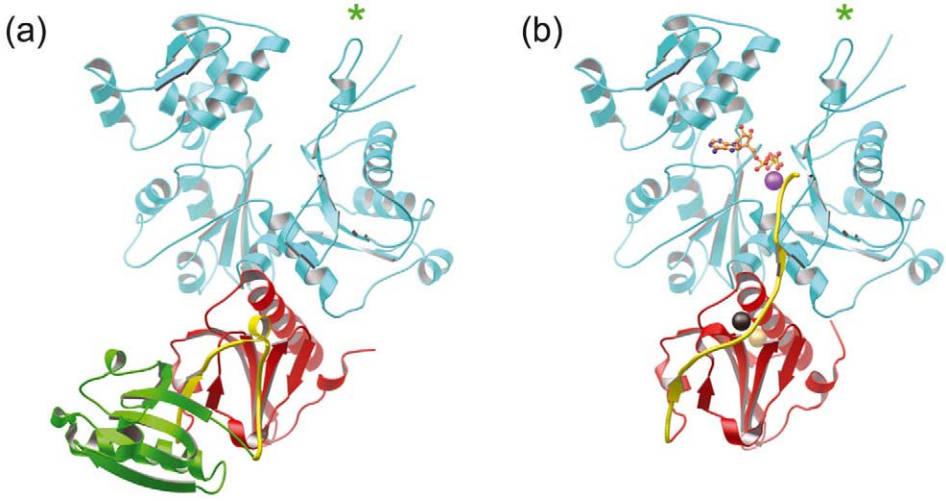

Fig. 1. Orientation of the G1–G2 linker prior to and after activation. The ribbon representation of actin is colored cyan, that of gelsolin G1 is red, that of gelsolin G2 is green, and the linker from G1 into G2 is gold. A green star indicates roughly the position at which G2 would be found if it contacted the next actin along the same strand in a filament. a: Domains G1 and G2 have been excised from the structure of inactive gelsolin [6] and G1 docked on to its binding site on actin [13]. Note the resulting location of G2 in this model. b: The structure at 2.6 Å resolution of the G1+ complex with actin. ATP is shown in a ball-and-stick representation and metal ions are depicted as spheres. The orientations of G1 and actin are approximately the same as in panel a. Note that the observed position of the linker would direct G2 approximately 130–140° clockwise from its position in panel a, i.e. toward the next actin unit in the direction of the pointed end of the filament in a two-start long-pitch helical model for F-actin.

DENZO and SCALEPACK [17]. A molecular replacement solution was found using the McLaughlin structure of G1/actin [13] (PDB ID 1EQY) within the program AMORE [18]. Repeated cycles of model rebuilding in O [19] and refinement in CNS [20] resulted in the current model. The structure was validated using PROCHECK [18], analyzed using CONTACT [18], and final refinement statistics are detailed in Table 1. There are no non-Gly residues in either disallowed or generously allowed regions of a Ramachandran plot. Figures were generated using MOLSCRIPT [21].

3. Results and discussion

3.1. Structure

The structure of the complex of G1+ with rabbit skeletal muscle actin, G1+/actin, refined at a resolution of 2.6 Å, shows the G1–G2 linker peptide extended up the surface of actin (Fig. 1b). In addition to G1+ and actin, ATP and four metal ions are evident. Three of the metal ions refine as Cd^{2+}, adjudged from the electron density and crystallographic *B*-factor refinement and consistent with the crystallization conditions. These include the one in close proximity to ATP (*B*-factor = 38.5 Å^2), the one sandwiched in the type-1 site [7] between actin and G1 (*B*-factor = 24.8 Å^2), and a novel metal-binding site sandwiched between adjacent actin units in the crystal packing (*B*-factor = 65.6 Å^2). The ion in the type-2 site [7] on G1 refines as Ca^{2+} (*B*-factor = 41.9 Å^2), which is in line with the reported non-exchangeable nature of this site [22]. G1+ buries 1383 Å^2 of actin's surface whilst actin–actin contacts in the crystal packing bury an additional 639 Å^2 on each actin.

Numerous close contacts are made between the extension residues Lys150 to Asn155 on G1+ and the linear stretch of actin residues from Asp24 to Val30. Hydrophilic interactions dominate and eight strong polar contacts are created (Fig. 2). For clarity, hydrophobic interactions are not shown in Fig. 2. These include a small pocket in which the side chain of Val152 from G1+ lies together with Ala26 and the stalks of the side chains of Arg28 and Asp24 from actin. A somewhat larger pocket includes Pro154 from G1+ and the side chains of Ala26, Val30 and Tyr337 from actin.

The space group of the complex ($P3_112$) differs from that of other G1/actin complexes, yet the polypeptide chains of the actin and G1 portions of the present and the previous [13] models are indistinguishable. The possibility of artifacts due to crystal packing, therefore, is reduced to a minimum for both. An interesting observation concerning the packing of protein within the G1+/actin crystals, which is mediated by Cd^{2+}, is illustrated in Fig. 3. At first glance, the actin–actin contacts in the pair of complexes shown bring to mind the end of an actin filament. However, this arrangement of the two actins relative to each other is not compatible with the

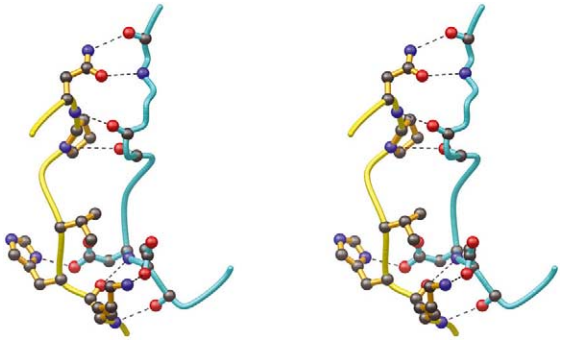

Fig. 2. A stereographic pair of images depicting the strong polar interactions between chain segment Lys150–Asn155 of gelsolin and segment Gly23–Val30 of actin. The backbone of actin is colored cyan, and that of gelsolin G1+ is yellow. For clarity, only those side chains that participate in polar interactions are depicted. Residues on the G1–G2 linker (in bold type) interact with the following actin residues (in italics), starting from the bottom of the diagram and working upward: **Lys150 (N)**, *Gly23 (O)*; **Lys150 (NZ)**, *Asp24 (OD1)*; **Lys150 (O)**, *Asp25 (N)*; **His151 (ND1)**, *Asp25 (OD2)*; **Pro154 (N)**, *Pro27 (O)*; **Asn155 (N)**, *Arg28 (O)*; **Asn155 (OD1)**, *Val30 (N)*; **Asn155 (ND2)**, *Val30 (O)*.

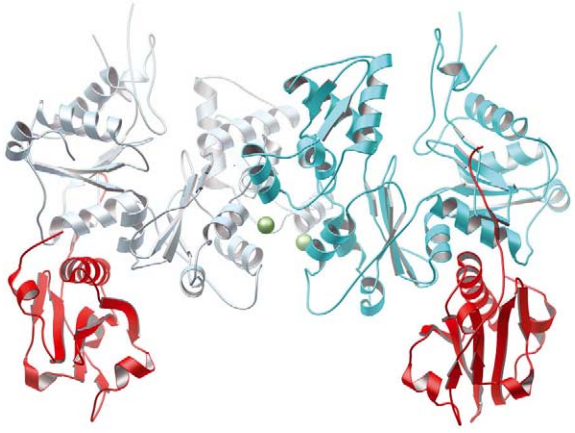

Fig. 3. Creation of an ion-binding site by actin–actin contact in the crystal packing. Ribbon representation of a pair of G1+/actin complexes in contact with each other in the crystal. A novel metal ion-binding site is created that involves participation of side chains Asp222 from one actin and Glu276 and Asn280 from the second.

Holmes [23], Lorenz [24], or Schutt–Lindberg [25] proposals for the structure of F-actin. We do not believe that the observed actin–actin crystal contacts are biologically significant.

3.2. Positioning of G2 on F-actin

The G1+/actin structure, if positioned within the Holmes model [23] for an actin filament, demonstrates that the linker to G2 leads towards the pointed end of the filament (Fig. 1b, towards the asterisk). In contrast (Fig. 1a), if the first two domains are excised from the Ca^{2+}-free structure of gelsolin [6] and G1 is docked to its binding site on actin, the G1 linker to G2 curves away from actin. Hence, in the inactive molecule, the G1–G2 linker adopts a completely different orientation, rotated some 130–140° away from that in the activated structure.

Gelsolin domain G2 is thought to bind to a site on an actin unit within F-actin in a manner that resembles the interaction between G1 and actin [10,26], as well as making contact with the same actin unit to which G1 ultimately binds [11,27]. Puius et al. [10] use this as the basis for a molecular model of how the first two domains of activated gelsolin bind to the barbed end of an actin filament. They began with the known G1/actin structure at a terminal position of the Lorenz representation of F-actin [24], then modeled activated G2 into the G1-binding site on the adjacent actin unit along the same long-pitch helix. A 10-residue linking peptide that fits snugly against actin spans the 30 Å gap between the C-terminus of G1 and the N-terminus of G2. Our crystallographic results provide proof for the last assumption.

In terms of the sequence of events that lead to severing, G2 approaches the side of an actin filament, making contact with two adjacent actin protomers longitudinally arranged on the same strand of a two-start helical representation of F-actin. Then, in a zipper-like manner, attachments form between the G1–G2 linker and actin, forcibly redirecting G1 to an insertion site one actin unit toward the barbed end of the filament from G2. Activation, therefore, results in large-scale repositioning of the domains of the first half of gelsolin relative to their locations in the inactive protein. Furthermore, the relative positions of the activated domains are distinct from those observed upon activation of the second half of gelsolin [7].

This mechanism of attachment of the G1–G2 linking peptide to actin may apply to other members of the gelsolin family of actin-binding proteins (Table 2). CapG, villin and advillin show clear homology in the actin-binding motif.

3.3. Analogy with WH2 domain proteins

Paunola et al. [28] performed a multiple sequence alignment of WH2 domain proteins to identify a common actin-binding motif. The stretch of residues of the gelsolin G1–G2 linker peptide that we observe to contact actin not only has analogs in other gelsolin family members, but more surprisingly resembles the most conserved actin-binding motif of the WH2 domain proteins. These include actin-binding proteins, such as WASp, WAVE (WASp family verprolin homologous protein) and WIP, that are involved in activation of the actin nucleating protein, arp2/3, and actin sequestering proteins, such as thymosin β4. Of particular interest is the pattern at the start of the motif of a hydrophobic residue followed by two basic residues, and then either Val or Thr (Table 2). Our structure infers that all of these proteins could interact with actin in a similar manner. Furthermore, an N-terminal residue of one WH2 protein, thymosin β4, cross-links to actin residue Glu167 [29], the identical residue to which the type-1 Ca^{2+} binds in this structure of G1+/actin. It seems plausible that the predicted N-terminal helix in the terminus of WH2 domains may occupy the groove between actin subdomains 1 and 2, akin to the main G1 helix, albeit with the opposite polarity. The mode of traversing from one end of an actin protomer to the other appears to have converged for families of actin-binding proteins involved in widely divergent functions that encompass actin-filament nucleation, severing, capping, and monomer sequestration.

Acknowledgements: We thank Therese Bergfors for crystallization facilities and Åke Engström for mass spectrometric analysis. We are grateful to the ESRF for provision of synchrotron radiation facilities and thank William Shepard for assistance in using beamline ID-29. For financial support, we thank the Swedish Natural Science Research Council (R.C.R.) and the Heart and Stroke Foundation of BC and the Yukon (L.D.B.). K.N. thanks the Swedish Foundation for International Cooperation in Research and Higher Education (STINT) for support through a grant to U.L.

Table 2
Comparison of the actin-binding site on gelsolin G1–G2 linker with analogous sequence segments in other gelsolin family members and with analogous regions on WH2 domain family members

Gelsolin family	Swiss-Prot Acc. No.	Sequence[a]
Gelsolin	(P06396)	F K H V X P N
Villin	(P09327)	M K H V X T N
CapG	(P40121)	F H K T X T G
Advillin	(O75366)	M K H V X T N
WH2 domain family		
Thymosin β_4	(P01253)	L K K T X T Q
Thymosin β_{10}	(P13472)	L K K T X T Q
WIP D1	(O43516)	L K K T X T N
WAVE 1	(Q92558)	L R K V X E Q
WAVE 2	(Q9Y6W5)	L R R V X E Q
WAVE 3	(Q9UPY6)	L K K V X E Q
CAP	(Q01518)	L K H V X D D
CAP2	(P40123)	L R H V X D D
N-WASp D1	(O00401)	L K K V X Q N
N-WASp D2	(O00401)	L K S V X D G
WASp	(P42768)	L N K T X G A

[a]X indicates an amino acid residue that does not contact actin.

References

[1] Pollard, T.D., Blanchoin, L. and Mullins, R.D. (2000) Annu. Rev. Biophys. Biomol. Struct. 29, 545–576.
[2] Loisel, T.P., Boujemaa, R., Pantaloni, D. and Carlier, M.F. (1999) Nature (London) 401, 613–616.
[3] Cunningham, C.C., Stossel, T.P. and Kwiatkowski, D.J. (1991) Science 251, 1233–1236.
[4] Sun, H.-Q., Yamamoto, M., Mejillano, M. and Yin, H.L. (1999) J. Biol. Chem. 274, 3319–33182.
[5] dos Remedios, C.G., Chhabra, D., Kekic, M., Dedova, I.V., Tsubakihara, M., Berry, D.A. and Nosworthy, N.J. (2003) Physiol. Rev. 83, 433–473.
[6] Burtnick, L.D., Koepf, E.K., Grimes, J., Jones, E.Y., Stuart, D.I., McLaughlin, P.J. and Robinson, R.C. (1997) Cell 90, 661–670.
[7] Robinson, R.C., Mejillano, M., Le, V., Burtnick, L.D., Yin, H. and Choe, S. (1999) Science 286, 1939–1942.
[8] Way, M. and Matsudaira, P. (1993) Curr. Biol. 3, 887–890.
[9] McGough, A., Chiu, W. and Way, M. (1998) Biophys. J. 74, 764–772.
[10] Puius, Y.A., Fedorov, E.V., Eichinger, L., Schleicher, M. and Almo, S.C. (2000) Biochemistry 39, 5322–5331.
[11] Renoult, C., Blondin, L., Fattoum, A., Ternent, D., Maciver, S.K., Raynaud, F., Benyamin, Y. and Roustan, C. (2001) Eur. J. Biochem. 268, 6165–6175.
[12] Choe, H., Burtnick, L.D., Mejillano, M., Yin, H., Robinson, R.C. and Choe, S. (2002) J. Mol. Biol. 324, 691–702.
[13] McLaughlin, P., Gooch, J.T., Mannherz, H.-G. and Weeds, A.G. (1993) Nature (London) 364, 685–692.
[14] Kwiatkowski, D.J., Janmey, P.A. and Yin, H.L. (1989) J. Cell Biol. 108, 1717–1726.
[15] Welch, M.D. and Mullins, R.D. (2002) Annu. Rev. Cell Dev. Biol. 18, 247–288.
[16] Spudich, J. and Watt, S. (1971) J. Biol. Chem. 246, 4866–4871.
[17] Otwinowski, Z. and Minor, W. (1997) Methods Enzymol. 276, 307–326.
[18] CCP4 (1994) Acta Crystallogr. D 50, 760–763.
[19] Jones, T.A., Zou, J.-Y., Cowan, S.W. and Kjeldgaard, M. (1991) Acta Crystallogr. A 47, 110–119.
[20] Brunger, A.T., Adams, P.D., Clore, G.M., DeLano, W.L., Gros, P., Grosse-Kunstleve, R.W., Jiang, J.S., Kuszewski, J., Nilges, M. and Pannu, N.S. et al. (1998) Acta Crystallogr. D 54, 905–921.
[21] Kraulis, P. (1991) J. Appl. Cryst. 24, 946–950.
[22] Weeds, A.G., Gooch, J., McLaughlin, P., Pope, B., Bengtsdotter, M. and Karlsson, R. (1995) FEBS Lett. 360, 227–230.
[23] Holmes, K.C., Popp, D., Gebhard, W. and Kabsch, W. (1990) Nature (London) 347, 44–49.
[24] Lorenz, M., Popp, D. and Holmes, K.C. (1993) J. Mol. Biol. 234, 826–836.
[25] Schutt, C.E., Myslik, J.C., Rozycki, M.D., Goonesekere, N.C.W. and Lindberg, U. (1993) Nature (London) 365, 810–816.
[26] Van Troys, M., Dewitte, D., Goethals, M., Vandekerckhove, J. and Ampe, C. (1996) FEBS Lett. 397, 191–196.
[27] Feinberg, J., Benyamin, Y. and Roustan, C. (1995) Biochem. Biophys. Res. Commun. 209, 426–432.
[28] Paunola, E., Mattila, P.K. and Lappalainen, P. (2002) FEBS Lett. 513, 92–97.
[29] Safer, D., Sosnick, T.R. and Elzinga, M. (1997) Biochemistry 36, 5806–5816.